Climate Smart Agriculture 1 (2024) 100005

Contents lists available at ScienceDirect

Climate Smart Agriculture

journal homepage: www.sciencedirect.com/journal/climate-smart-agriculture

Regular Article

Assessing flood-depth effects on water quality, nutrient uptake, carbon sequestration, and rice yield cultivated on Histosols

Yuchuan Fan [a], Naba R. Amgain [b], Abul Rabbany [c], Noel Manirakiza [c,d], Xue Bai [c,d], Matthew VanWeelden [c], Jehangir H. Bhadha [c,d,*]

[a] Mississippi State University Geosystems Research Institute, Starkville, MS, 39759, USA
[b] Purdue University, Department of Horticulture & Landscape Architecture, West Lafayette, IN, 47907, USA
[c] University of Florida, Everglades Research and Education Center, 3200 E Canal St. S, Belle Glade, FL, 33430, USA
[d] University of Florida, Soil, Water and Ecosystems Sciences Department, Gainesville, FL, 32611, USA

ARTICLE INFO

Keywords:
Continuous flood irrigation
Hydrologic budget
Water quality index
Climate change
Soil health

ABSTRACT

In the Everglades Agricultural Area (EAA), Florida, cultivating rice in flooded paddies is becoming increasingly popular to conserve water and soil health. Flood depth is a critical factor affecting the discharged water quality, soil carbon, and yield production. However, few studies have comprehensively investigated the optimal flood depth in EAA, considering multi-functional indices. To address this gap, we investigated drainage water quality, water quantity, nutrient uptake, soil carbon, and rice yield in rice paddies in histosol soils over a two-year period at four flood depths (5, 10, 15, and 20 cm). For each flood depth, averaged over two years, total outflow loadings of suspended solids, nitrogen, phosphorus, and potassium were significantly reduced by 40 %, 38 %, 36 %, and 32 %, respectively, compared to inflow water loadings ($p < 0.001$). Soil organic carbon (SOC) in 5, 10, 15, and 20 cm flood treatments increased annually at a rate of 3.85 %, 5.64 %, 6.86 %, and 6.86 %, respectively; for these same treatments, soil active organic carbon (AOC) decreased annually at rates of 11.75 %, 8.63 %, 20.07 %, and 8.48 %, and rice grain yield was 4488, 5103, 5450, and 5386 kg ha^{-1}, respectively. Overall, considering the water quality, SOC, AOC, and rice yield production, irrigating rice paddies at a flood depth of 15 cm most effectively improves water quality, increases carbon sequestration, reduces active carbon, and yields more rice than other flood depths. By evaluating the effects of flood depth on the soil–water–plant nexus in a holistic manner, we propose a more sustainable and environmentally friendly mode of rice cultivation within the EAA.

1. Introduction

Rice (*Oryza sativa* L.) is a primary staple crop, integral to the diets of over 1.6 billion people worldwide [1]. In the Everglades Agricultural Area (EAA) of South Florida, rice has been a key rotational crop alongside sugarcane during the late spring and summer months since 1977, covering approximately 24,000 acres in 2021 [2]. In this region, the preference for cultivating rice over managing flooded fallow fields has been well-documented due to its economic importance and beneficial impacts on environmental ecosystems [3,4].

The EAA has faced significant environmental challenges, notably nutrient losses from non-point sources and soil carbon oxidation, which have been prevalent issues over the past two decades [2,5]. Particularly, soil subsidence, occurring at a rate of approximately 0.64 cm per year due to the oxidation and decomposition of soil organic matter in the highly organic histosols, exemplifies these challenges [6]. Furthermore, the annual discharge of approximately 1110 million m^3 of water from the EAA underscores the necessity for enhanced drainage water quality to sustain agricultural productivity and local ecosystems [7].

In response, rice cultivation in flooded paddies offers a promising solution. This method not only reduces soil carbon oxidation by creating a physical barrier that inhibits weed germination and microbial activity—thus preserving soil organic matter—but also mitigates nutrient losses from non-point sources. Specifically, flooding increases nutrient availability in the vadose zone by desorbing nutrients from soil colloids, which is critical for maintaining soil fertility without the need for added N, P, and K fertilization [5,8]. This is particularly beneficial in the EAA, where the inherent richness of highly organic histosol soils, combined with nutrient-enriched water pumped from local canals, naturally sustains crop growth. Consequently, flooded rice cultivation plays a crucial

* Corresponding author. University of Florida, Everglades Research and Education Center, 3200 E Canal St. S, Belle Glade, FL, 33430, USA.
E-mail address: jango@ufl.edu (J.H. Bhadha).

https://doi.org/10.1016/j.csag.2024.100005
Received 19 March 2024; Received in revised form 6 June 2024; Accepted 6 June 2024

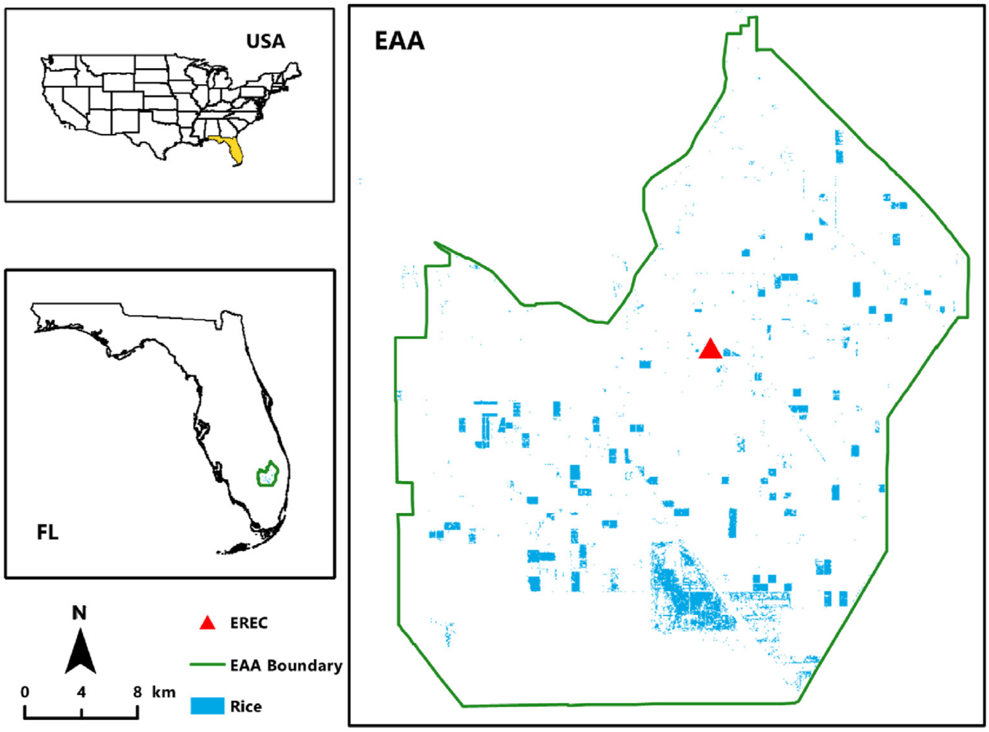

Fig. 1. Map displaying geographic locations of Everglades Research and Education Center (EREC) in Everglades Agricultural Area (EAA), along with the distribution of flooding rice in Florida based on the USDA cropland data layer of 2021 https://nassgeodata.gmu.edu/CropScape/.

role in mitigating nutrient losses and soil carbon oxidation, thereby enhancing the sustainability of agricultural practices in the region.

While the benefits of flooded cultivation are apparent, one specific management factor has been overlooked—flood depth. As a matter of fact, flood depth plays a crucial role in various aspects of rice cultivation, including rice growth, soil carbon, nutrient uptake, and water quality [5,9]. It was reported that the significant impact of flooding depth and duration on the growth traits and yield of rice [10], and existing an optimal depth for maximal production [11] and high-quality rice [9]. Regarding nutrient uptake, flood depth can impact rice plants' ability to absorb nutrients. It was found that under non-flooded irrigation conditions, rice plants adapted by increasing root/shoot ratio and root length density at specific soil depths, indicating a response to altered water availability [12]. This adaptation demonstrates how flood depth variations can influence nutrient uptake mechanisms in rice plants, leading to improved water quality through reduced nutrient discharge [5]. In conclusion, flood depth is a critical factor affecting rice cultivation, with implications for nutrient losses, soil carbon sequestration, and rice yield. Understanding the relationship between flood depth and these aspects is crucial for optimizing rice production in diverse environmental conditions.

However, there is no consensus about optimal flood depth considering multi-functional indices in the EAA. Most studies that have examined flooded rice cultivation have focused on the single benefits of this form of agriculture, as opposed to its effects on multiple ecological variables. To address this gap, in this study, nutrient concentration, soil carbon sequestration, and yield production are considered as multi-indices to be considered to evaluate the optimal flood depth in the EAA. In most cases, flood depth in the EAA ranges from 5 to 20 cm [9,11]. Therefore, for more sustainable agricultural management to harmonize productivity with environmental stewardship, we (i) analyze the impact of different flood depths (5, 10, 15, and 20 cm) on water quality and outflow discharge; (ii) evaluate nutrient uptake and soil carbon dynamics at different flood depths; and (iii) identify an optimal flood depth by balancing non-point source losses, soil carbon sequestration, and rice yield. This research contributes to climate-smart agriculture by proposing practices that improve rice cultivation sustainability and efficiency, and align with broader environmental and climate-related objectives.

2. Material and methods

2.1. Experimental design

Rice was grown at a University of Florida experimental plot within the EAA (80°37′55″W, 26°40′3″N) in farmland managed by the Everglades Research and Education Center (EREC) (Fig. 1). The region experiences a tropical climate with an average rainfall of 1330 mm, and an average temperature of 24 °C [13]. Sixteen plots (83.8 m × 18.3 m = 1533 m^2) were planted with a common commercial rice variety Diamond (long-grain, short-season), at 95 kg ha^{-1} during the summers of 2019 and 2020. Plots were leveled before planting, and dry-seeded. No fertilizer was applied. Each of the four flood depth treatments was replicated four times (Fig. S1), including 5 (FD5), 10 (FD10), 15 (FD15), and 20 cm (FD20).

2.2. Water management and balance calculation

Irrigation water was pumped by an electric pump from a northern canal. The inflow valve and riser boards controlled the water depth in each plot in the outflow box (Fig. S1). All plots were separated by a 6 m wide levée (bund). For each treatment, the inflow water rate (V_{in}, $m^3\ h^{-1}$) was recorded by estimating the volume of water per unit time. The outflow water rate (V_{out}, $m^3\ h^{-1}$) was calculated by measuring the water flow rate (m h^{-1}) through a portable flowmeter (Model 2000, Marsh-McBirney Inc, USA), and multiplying the cross-sectional area (m^2) of the outflow pipe. The flow rate was measured daily. To ensure a flood depth within the 5–20 cm range, the valve was opened and the pump was run for 5 h every 2 d; the valve remained open until the desired flood depth was achieved. The outflow contributes significantly to water loss; water inflow (I) and outflow (O) ($m^3\ ha^{-1}\ d^{-1}$) are calculated as follows:

$$I = V_{in} \times T \times \frac{10000}{A} \quad (1a)$$

$$O = V_{out} \times T \times \frac{10000}{A} \quad (1b)$$

where V_{in} *and* V_{out} represent inflow and outflow water rate (m^3 $hour^{-1}$); T represents the inflow or outflow running time (hour); A represents the area of each independent plot (m^2); the constant 10,000 represents the area of 1 ha.

To calculate the water budget, a water balance method was applied to understand water in- and outflow components. Inputs include irrigation (inflow) and rainfall, and outputs include discharge (outflow), seepage, and evapotranspiration (ET). The pump flow rate and duration of pumping can be used to calculate inflow. Meteorological data were obtained from the Florida Automated Weather Network (FAWN, https://fawn.ifas.ufl.edu), with a weather station in Belle Glade, 50 m from the plots (rainfall and temperature data) (Fig. S2). Crop evapotranspiration (ET_C) was calculated using the Penman-Montieth equation [14] as follows:

$$ET_C = K_C \times ET_O \quad (2a)$$

where K_C represents the crop coefficient. Daily rice evapotranspiration (ET_D, m^3 ha^{-1} d^{-1}) was calculated as follows:

$$ET_D = ET_C \times \frac{24}{0.25} \times \frac{10000}{1000} \quad (2b)$$

Seepage (S, m^3 ha^{-1} d^{-1}) was calculated using the water balance equation:

$$I + P = ET_D + \Delta S + O \quad (2c)$$

where I is irrigation (inflow water, m^3 ha^{-1} d^{-1}), P is precipitation (m^3 ha^{-1} d^{-1}), ET_D is rice evapotranspiration (m^3 ha^{-1} d^{-1}), ΔS is the change of seepage (m^3 ha^{-1} d^{-1}), and O is runoff (outflow water, m^3 ha^{-1} d^{-1}).

2.3. Sample collection and analysis

Water samples were periodically (every two to three days) collected from inflow and outflow waters three weeks after planting, once the flood depth had stabilized for both the 2019 and 2020 growing seasons (June–September). All water samples were collected in polyethylene bottles, stored at 4 °C, and transported to the Soil, Water, and Nutrient Management laboratory (EREC, Belle Glade) for analysis. Each year (Fig. S3), total suspended solids (TSS) were measured using EPA method 160.2, where 500 ml of sample was poured through a vacuumed magnetic filtration system equipped with a 47 mm Whatman 934-AH glass microfiber filter; the filter was then carefully removed from the top of the magnetic filtration system and placed in an aluminum weighing dish that contained it before filtration, which was then placed into an oven to dry at 105 °C for 24 h, then placed into a desiccator to cool for at least 30 min. The change in mass divided by the volume corresponds to the TSS (mg L^{-1}). TN was measured in water samples using a Shimadzu Total Organic Carbon Analyzer (TOC-L) with the TNM-L module combustion method. The combustion furnace temperature was maintained at 720 °C with an air carrier gas flow rate of 150 ml min^{-1}. A 20 μl sample was directly injected into the combustion furnace column using a Shimadzu autosampler, and the detected outcome result was measured in mg L^{-1}. Total phosphorus (TP) and TK were measured in water samples using EPA method 200.7 by Agilent Inductively Coupled Plasma Optical Emission Spectroscopy (ICP-OES) 5110 at a 213.618 nm wavelength (TP) and 766.491 nm (TK).

Inflow and outflow (INL and ONL, kg ha^{-1} d^{-1}) nutrient loading per plot were calculated as follows:

$$INL_i = IC_i \times I \quad (3a)$$

$$ONL_i = OC_i \times O \quad (3b)$$

where IC_i represents the i_{th} parameter of inflow concentration, mg L^{-1}; OC_i represents the i_{th} parameter of outflow concentration, mg L^{-1}; and I and O represent the volume of inflow and outflow (m^3 ha^{-1} d^{-1}).

2.4. Water quality index

The Canadian Council of Ministers of the Environment (CCME) water quality index (WQI) was used to evaluate outflow water quality at different flood depths. This index is widely used to assess surface water quality because of its ease of application and flexibility in choosing water quality indicators; it requires a minimum of four water quality indicators as model inputs. We selected five inputs (pH, TSS, TN, TP, TK) to evaluate outflow water quality for each flood depth. According to local water management district rules, the maximum objective values for pH, TSS, TN, TP, and TK are 6.5–8.4, 2000 mg L^{-1}, 10 mg L^{-1}, 0.01 mg L^{-1}, and 2 mg L^{-1}, respectively [15]. CCME WQI is calculated following [16]:

$$WQI = 100 - \left[\frac{\sqrt{F_1^2 + F_2^2 + F_3^2}}{1.732}\right] \quad (4a)$$

$$F_1 = \left[\frac{\text{number of failed parameters}}{\text{total number of parameters}}\right] \times 100 \quad (4b)$$

$$F_2 = \left[\frac{\text{number of failed tests}}{\text{total number of tests}}\right] \times 100 \quad (4c)$$

$$F_3 = \left[\frac{\text{nse}}{0.01(\text{nse}) + 0.01}\right] \quad (4d)$$

$$nse = \left[\frac{\sum_{i=1}^{n} excursion_i}{total\ number\ of\ test}\right] \quad (4e)$$

If a test value falls below the objective value, the excursion for that test value is calculated as follows:

$$excursion_i = \left[\frac{failed\ test\ value_i}{Objective_j}\right] - 1 \quad (4f)$$

Conversely, if the test value exceeds the objective value, the excursion value is calculated as follows:

$$excursion_i = \left[\frac{Objective_j}{failed\ test\ value_i}\right] - 1 \quad (4g)$$

where F_1 is termed the “scope,” F_2 is the “frequency,” and F_3 is the “amplitude.” This is calculated by an asymptotic function that scales the normalized sum of excursions (nse) of test values from objectives to yield a value between 0 and 100. The CCME model proposed five water quality classes: excellent (WQI = 95–100), good (WQI = 80–94), fair (WQI = 65–79), marginal (WQI = 45–64), and poor (WQI = 0–44).

2.5. Soil carbon

Soil samples were collected before rice planting (pre-planting, 4/19/2019 and 5/11/2020) and after harvest (post-harvest, 8/29/2019 and 9/18/2020). Each sample was collected from the top 15 cm of the soil. Active organic carbon (AOC) was measured by Thermo Scientific Genesys 30 spectrophotometer at 550 nm [17]. Soil organic carbon (SOC) was analyzed using the loss on ignition method [18].

2.6. Statistical analyses

Water concentration and nutrient loads were estimated for the 2019

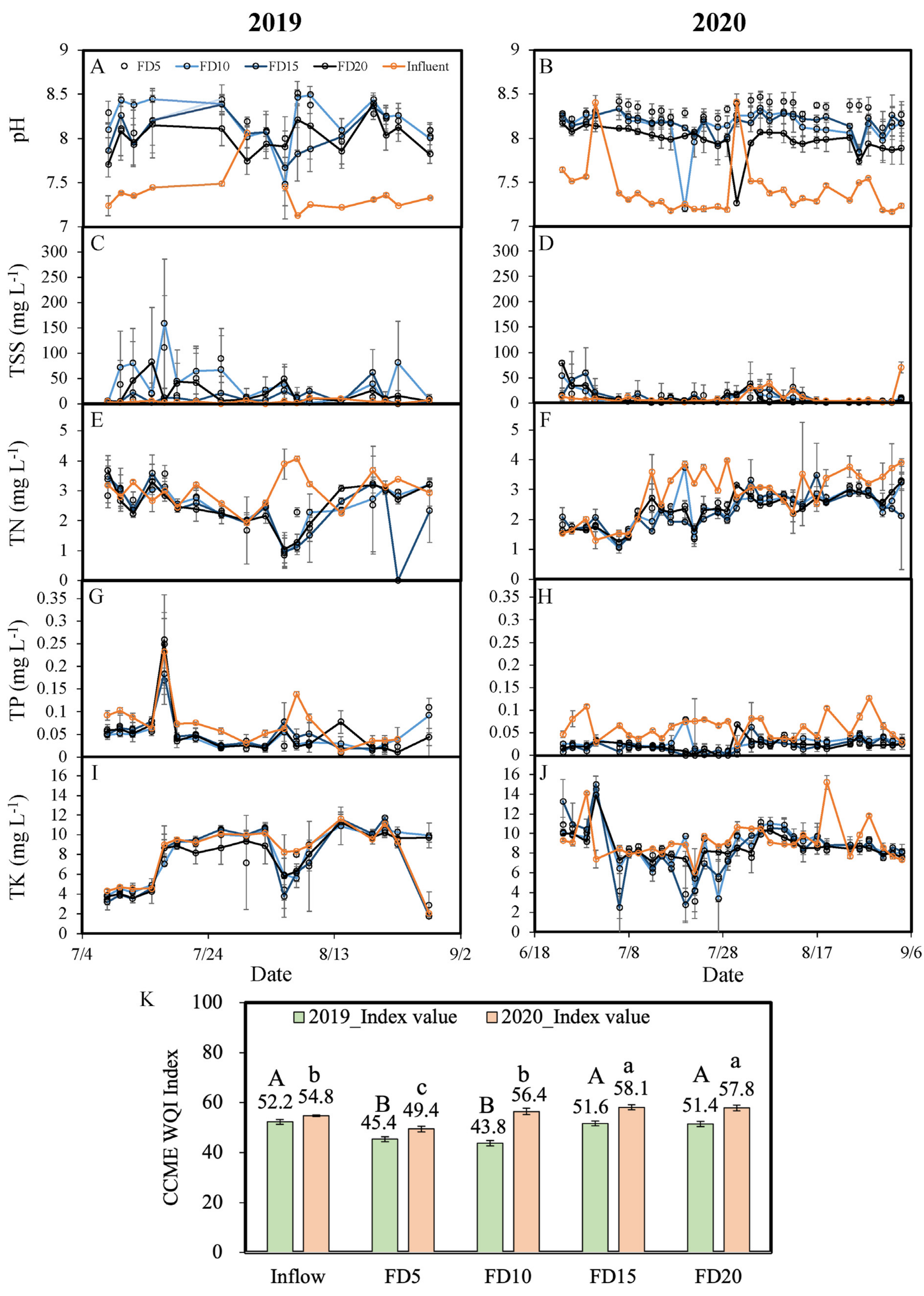

Fig. 2. The concentrations of (A, B) pH, (C, D) total suspended solids (TSS), (E, F) total nitrogen (TN), (G, H) total phosphorus (TP), and (I, J) total potassium (TK) were calculated in inflow and outflow at 5, 10, 15, and 20 cm of flood depth in 2019 and 2020, respectively. The bar represents the standard deviation. The water quality index (WQI) of outflow under different flood depths, including 5 cm (FD5), 10 cm (FD10), 15 cm (FD15), and 20 cm (FD20). (K) Canadian Council of Ministers of the Environment (CCME) WQI model comprehensively evaluates the inflow and outflow values. The uppercase and lowercase letters represent the significant difference between the flood depths in 2019 and 2020, respectively ($p < 0.05$).

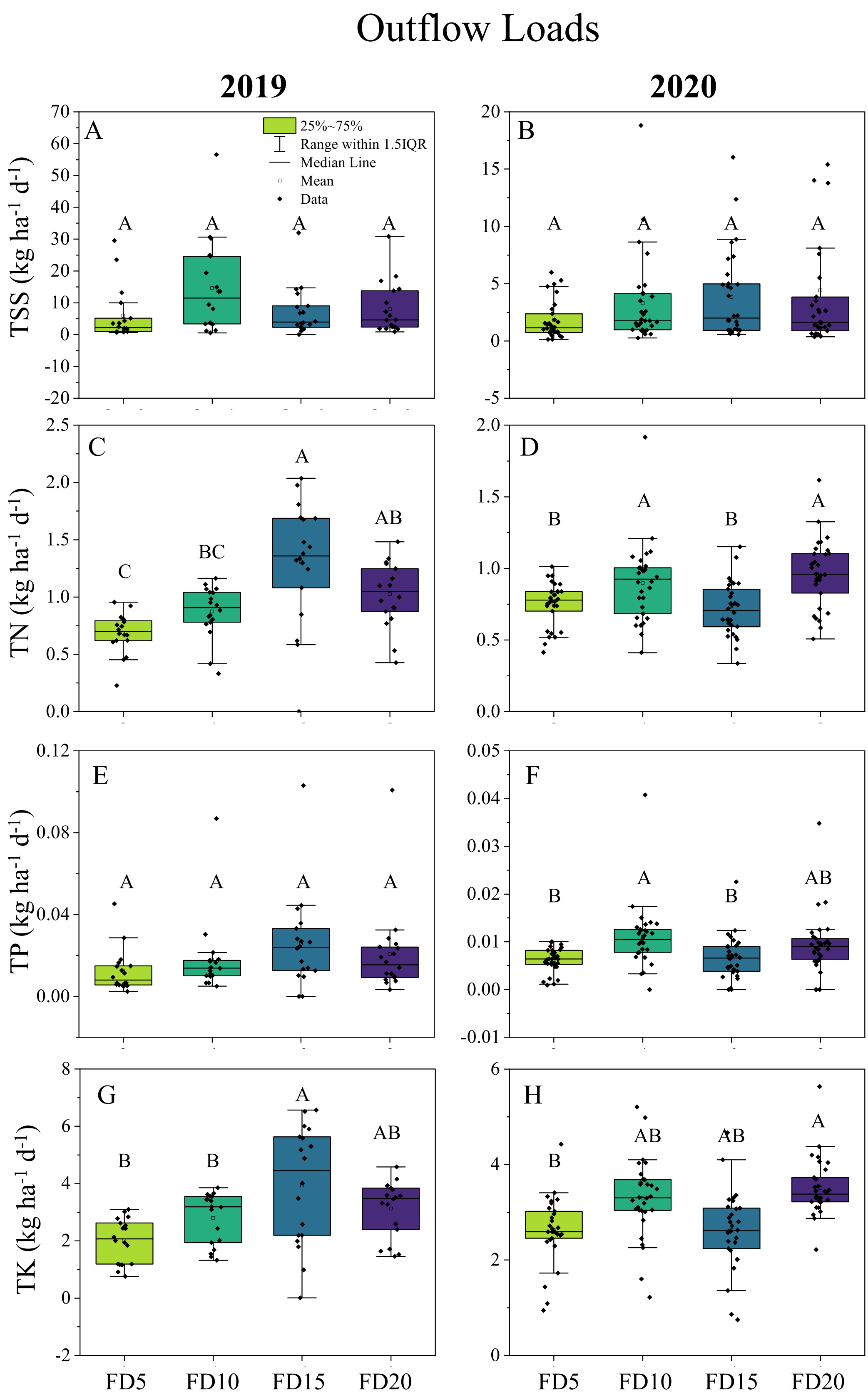

Fig. 3. (A–B) Total suspended solids (TSS), (C–D) total nitrogen (TN), (E–F) total phosphorus (TP), and (G–H) total potassium (TK) concentration measured in inflow and outflow at 5 (FD5), 10 (FD10), 15 (FD15), and 20 (FD20) cm of flood depth in 2019 and 2020. The error bar represents the standard deviation. The uppercase letters represent a significant difference at $p < 0.05$. * represents significant change ($p < 0.05$); *** represents extremely significant change ($p < 0.001$).

and 2020 rice growing seasons. ANOVA was used to identify significant differences in water quality indicators, TP, and TK concentrations, in shoot and root tissues among the four flood depths. Statistically significant differences between inflow and outflow loads were estimated using Student's T-tests with post hoc (Tukey's HSD) in SPSS (IBM Inc, SPSS 27, USA). All figures were prepared using Origin (OriginLab Inc, 2021b, USA) and Excel (Microsoft Inc, 2022, USA). Data were analyzed separately for each year when results differed significantly ($p < 0.05$).

A structural equation model was fitted to infer the relative importance of flood depth on water quality, nutrient use efficiency, and crop growth indicators (AMOS 26; IBM Corporation, Meadville, PA, USA). The Normed Fit Index and Root Mean Square Error of Approximation were used as indicators to evaluate the fitting degree of the model [19,20]. For the structural equation model, the standardized path coefficients (SPC) indicate the direct effect of a variable assumed to be a cause on another variable considered an impact. A greater SPC (close to 1) means this effect is relatively high, and the plus or minus represents the positive or negative relationship between variables.

3. Results

3.1. Water quality and outflow loads

The in- and outflow water quality were measured during the growth season as shown in Fig. 2A–J. For pH and TSS, the outflow showed a greater value than the inflow in most water samplings. While for TN, TP, and TK, there is a significant reduction in outflow compared with inflow in most cases. To quantitatively evaluate the change in the water quality, the CCME WQI model was evaluated in in- and outflow water quality. WQI values for in- and outflow at FD5, FD10, FD15, and FD20 were 52.9, 46.3, 44.0, 52.6, and 52.3 for 2019, respectively (Fig. 2K). Compared with inflow WQI, FD5 and FD10 were significantly lower WQI ($p < 0.05$), but there was no significant change between FD15 and FD20. In 2020, values were 54.7, 50.2, 56.2, 58.5, and 57.3, which were slightly lower than 2019 (Fig. 2K). Compared with inflow WQI, the WQI at 5 cm was significantly lower ($p < 0.05$), there was no significant change at FD10, but WQI at FD15 and FD20 was significantly greater ($p < 0.05$). In most cases, values represented a marginal range (45–64), and at FD15 and FD20, WQI values were greater than at FD5 and FD10.

Nutrient loads were estimated as a product of the water quality indicator and volume of water. Nutrient loads for TSS, TN, TP, and TK are shown in Fig. 3A–H. Flood depths have no impact on the TSS outflow loading (Fig. 3A and B). In terms of TN loading, FD15 and FD20 show greater value than FD5 and FD10 in the first year (Fig. 3C), while the TN loading of FD15 reduced significantly in the second year (Fig. 3D). For TP loading, there is no significant difference in the first year (Fig. 3E), while it shows FD5 and FD15 had lower loading than FD10. In terms of TK, FD15 shows greater value than FD5 and FD10 in the first year (Fig. 3G), while FD15 has no significant difference with other flood depths in the second year (Fig. 3H).

3.2. Flooded rice impacts on SOC and AOC

As shown in Fig. 4A, soil organic carbon (SOC) levels were relatively stable in 2019, but notably increased in 2020. In contrast, active organic carbon (AOC) reduced markedly in 2019, then stabilized, with no significant increase in 2020 (Fig. 4B). Moreover, over both years, average annual SOC values for FD5, FD10, FD15, and FD20 are 448.8, 468.8, 439.0, and 468.1 g kg^{-1}, respectively; for these same treatments, AOC values were 21.6, 20.9, 21.8, and 22.5 g kg^{-1}, respectively.

3.3. Comparison of water quality, water quantity, soil carbon, and yield production under different flood depths

A radar chart prepared to visually compare the performance of various flood depths across multiple evaluation indices over two years is presented in Fig. 5. These indices encompass the SOC increase rate (%), yield (kg ha^{-1}), water consumption (m^3 ha^{-1} d^{-1}), WQI change rate (%), and AOC decrease rate (%). This approach improves our understanding of the effects of different flood depths on agricultural productivity and environmental sustainability.

A higher SOC percentage corresponds to a more significant accumulation of organic carbon in the soil, and enhanced soil fertility and carbon sequestration capabilities. FD15 and FD20 have the highest SOC increase rate (6.86 %), surpassing rates for FD10 (5.64 %) and FD5 (3.85 %) (Fig. 5). The rate of decrease in AOC indicates the soil's potential to

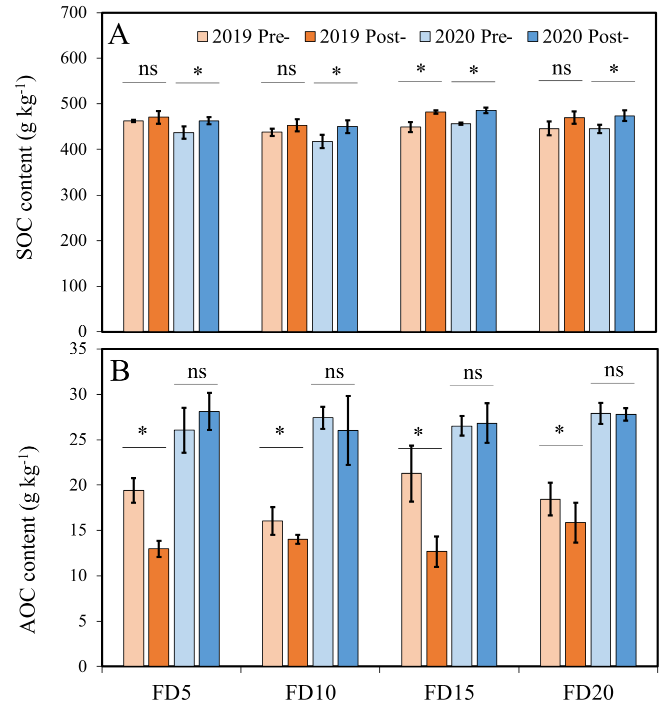

Fig. 4. The comparison of soil indicators, including A) soil organic carbon (SOC, g kg^{-1}) and B) active organic carbon (AOC, g kg^{-1}) at pre-planting and post-harvest at 5 (FD5), 10 (FD10), 15 (FD15), and 20 (FD20) cm of flood depth. The *ns* letter indicates no significant difference between the pre-planting and post-harvest ($p < 0.05$). The error bar indicates the standard deviation.

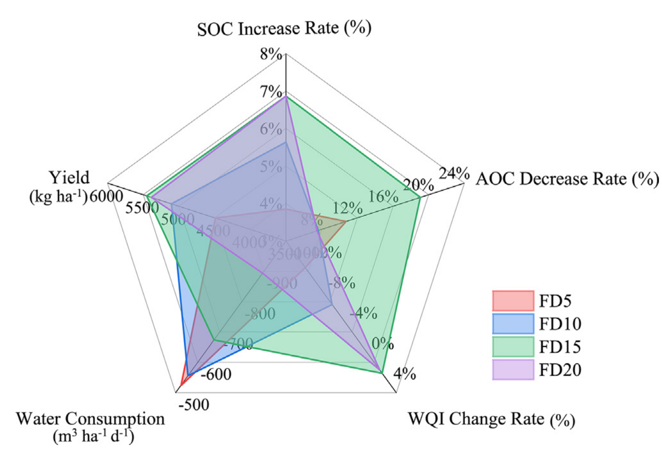

Fig. 5. The radar chart of different flood depth performance at five different indices, including soil organic carbon (SOC) increase rate (%), yield (kg ha^{-1}), water consumption (m^3 ha^{-1} d^{-1}), water quality index (WQI) change rate (%), and active organic carbon (AOC) decrease rate (%). The red area represents the 5 cm flood depth (FD5), the blue area represents the 10 cm flood depth (FD10), the green area represents the 15 cm flood depth (FD15), and the purple area represents the 20 cm flood depth (FD20).

reduce greenhouse gas emissions, with a higher rate signifying reduced soil AOC retention. The highest decrease rate (20.07 %) occurred at FD15, then FD5 (11.75 %), FD10 (8.63 %), and FD20 (8.48 %), suggesting that flood depth affects soil carbon dynamics (Fig. 5).

A positive WQI value indicates improved water quality from the inflow to outflow. WQI values were greatest at FD15 (2.43 %), then FD20 (1.99 %), FD10 (2.43 %), and FD5 (−11.49 %), indicating differential effects of flood depth on water quality. Water usage progressively decreased from FD20 to FD5 (Fig. S4).

Yield at FD5, FD10, FD15, and FD20 flood depth was 4488, 5103, 5450, and 5386 kg ha^{-1}, respectively. Yield was highest at FD15, indicating that certain flood depths can optimize agricultural output despite variations in environmental indices.

Overall, a flood depth of FD15 emerges to be optimal, with superior performance across several indices and its predominant representation on the radar chart. This indicates the importance of optimizing flood depth to balance agricultural productivity with environmental stewardship and provides valuable insights for agricultural water-management strategies.

4. Discussion

Flooded rice cultivation significantly affects concentrations and loads of TSS, TN, TP, and TK in the outflow. Therefore, a WQI value based on these parameters varies at different flood depths. Of measured variables, TP most affects WQI, consistent with previous studies that have reported that flooded rice reduced P [4,5,21]. However, despite there being no significant difference in outflow TP concentration for different flood depths, significant differences in TP loads between inflow and outflow occurred ($p < 0.05$). At 15 cm, WQI was greater than at other flood depths, probably because more water samples collected in FD15 were below the TP criterion (0.01 ppm). Results indicate that reduced TP load was observed at a lower flow rate because both TP (C_{TP}) and TSS (C_{TSS}) concentrations correlated highly with flood depth. The Pearson correlation coefficient for C_{TP} and C_{TSS} is 0.62 at FD, and 0.64 at FD10 ($p < 0.05$) (Fig. 6). In contrast, Pearson correlation coefficients between C_{TP} and C_{TSS} at FD15 and FD20 are 0.037 and 0.079, respectively (Fig. 6). This indicates a stronger relationship between C_{TP} and C_{TSS} at lower flood depths, possibly because: (1) lower flood depth increases water velocity, as explained by Manning's equation, where water velocity is inversely proportional to flow area [22]; this can increase suspended particles and SOC from the soil surface, and release more particulate P into the outflow. Alternatively, (2) greater velocity at shallow depth reduces water residence time [23], resulting in lower P uptake by rice.

A more significant relationship occurred between outflow TN concentration (C_{TN}) and C_{TP} at lower flood depth. This correlation coefficient decreased with increasing flood depth (Fig. 6), possibly contributing to increased concentration of C_{TN} at lower flood depth. Increased C_{TP} at lower flood depths may be because of reduced residence time, and limited bioavailable P taken-up by rice roots. Shallow flood depth may also result in more N in flood water by three pathways: (1) through soil (histosol) loss in the EAA, inherently rich in N (up to 2 % N) [24]; (2) greater velocity of water at low flood depth, decreasing bioavailable N uptake by rice roots, as for P (because of limited residence time); and (3) denitrification, as a pathway of N loss from flood water [25]. However, shallow flood depth will hamper denitrification because dissolved oxygen content is high, thereby reducing N loss [19,20].

Overall, flood depth may impact water quality through complex physical, chemical, and microbial processes. We examined only pH, TSS, TN, TP, and TK to assess water quality because rice cultivation in the EAA requires no N, P, or K fertilizer [26]. However, different water and fertilizer management regimes may produce different results. Shallow irrigation and a deep-sluice with new N management could decrease TN and TP loss from runoff leaching compared with continuous flooding irrigation with common N fertilization practices [27]. Also, optimizing N input could reduce N loss [28], and alternating wetting and drying increased nitrate leaching loss compared with continuous flooding irrigation [29].

Flooded rice cultivation has been shown to significantly impact soil carbon sequestration, leading to a greater SOC increase rate and a lower AOC decrease rate at the FD15. Previous studies reported the potential mechanism of flood depth influencing soil carbon sequestration is attributed to the assimilation and distribution of carbon in shoots and roots [30]. However, our study didn't find any significant difference in the carbon root shoot ratio among different flood depths. Thus, we infer that the differences in SOC and AOC are not caused by the distribution of carbon in shoots and roots. Instead, they may be influenced by the

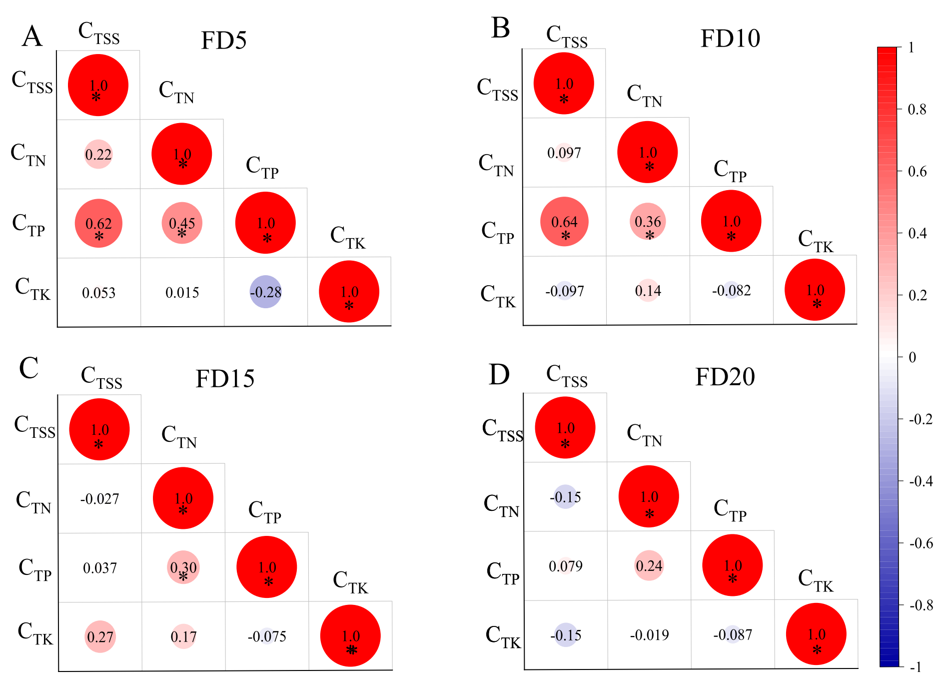

Fig. 6. Pearson correlations between the concentrations of outflow TSS, TN, TP, and TK at A) 5 cm (FD5), B) 10 cm (FD10), C) 15 cm (FD15), and D) 20 cm (FD20) of flood depth. * represents a significant difference ($p < 0.05$).

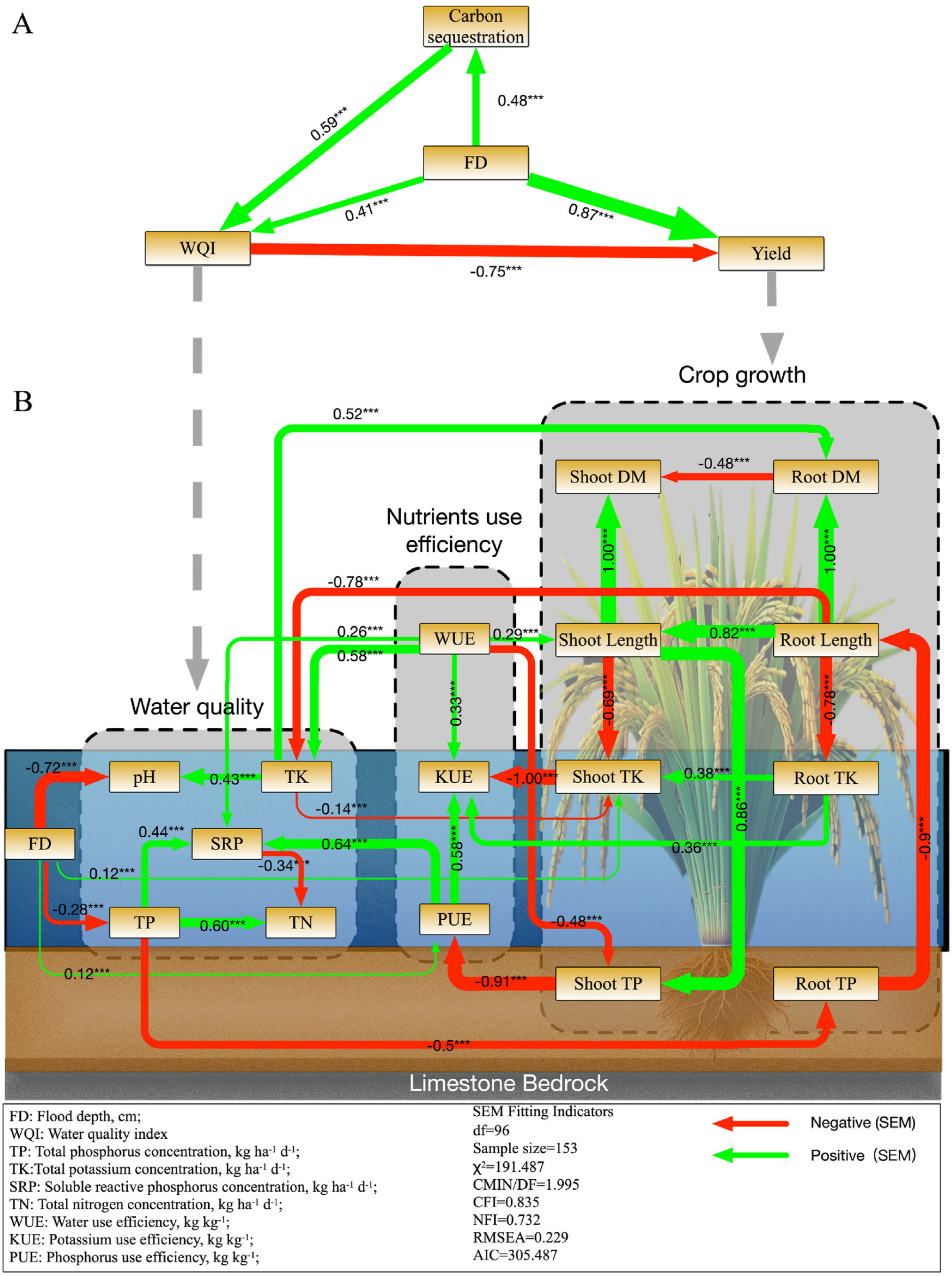

Fig. 7. Structural equation modeling for understanding the continuous flooding irrigation impact on water quality, nutrient use efficiency, shoot and root properties. Boxes indicate variables. An arrow represents a causal relationship. The Arrow direction indicates the direction of effect. The arrow width indicates effect size. A green arrow denotes a positive relationship, and a red arrow denotes a negative relationship. The numbers above the arrows are standardized path coefficients (*SPC*). * represents $p < 0.05$; ** represents $p < 0.01$; *** represents $p < 0.001$.

chemical and physical reactions between soil and floodwater.

Moreover, the depth of flooding influences yields indirectly. There are many reasons attributed to the difference. For example, the panicle initiation stage can increase rice plant height after flooding, and elongation of the internodes is faster underwater than in the air [31] (Fig. S5). However, flooding decreases the photosynthetic apparatus in rice fields [32] and may damage the plant [10]. Thus, shallow (<5 cm) or deeper flood depth (>15 cm) might not be optimal, and a more optimal depth may exist between them. Likewise, it was investigated various pond depths (0, 3, 6, 9, 12, 15, and 18 cm) on paddy rice growth and yield, and determined 9 cm to be optimal for production under continuous and intermittent irrigation [11]. Also, it was reported that flood depths of 2, 8, 12, 15, and 18 cm on rice grain quality, and recommended a flood depth of 10 cm for high-quality rice [9]. Thus, rice yield can be attributed to different factors [1]. We suggest an optimal flood depth of 15 cm for rice yield, which is higher than previous studies. This inconsistency may be because we consider more factors (non-point source nutrient losses, soil carbon sequestration, and rice yield production) rather than a single objective. Conversely, we infer that variance in optimal flood depth may be associated with fertilizer conditions [33]. However, because fertilizer was not required to cultivate rice in the EAA, this greater flood depth may be required to obtain more nutrients from influent water to maximize yield.

To better understand the interrelationships of flood depth with water quality, carbon sequestration, and crop yield, a structural equation modeling analysis was done as shown in Fig. 7A, flood depth positively correlates with WQI (SPC = 0.41, $p < 0.001$), carbon sequestration (SPC = 0.48, $p < 0.001$), and yield (SPC = 0.87, $p < 0.001$). Also, carbon sequestration positively correlates with WQI (SPC = 0.59, $p < 0.001$). However, WQI negatively correlates with yield (SPC = −0.75, $p < 0.001$), which indicates there is a trade-off between WQI and yield. Therefore, Fig. 7B presents how flood depth affects water quality directly and indirectly by influencing nutrient use efficiency and crop growth and altering the nutrient composition of floodwater. Specifically, flood depth mainly affects water quality indicators such as pH (SPC = −0.72, $p < 0.001$) and TP (SPC = −0.28, $p < 0.001$). An increase in TP positively correlates with SRP (SPC = 0.44, $p < 0.001$) and TN (SPC = 0.60, $p < 0.001$), but correlates negatively with root TP (SPC = −0.50, $p < 0.001$). Therefore, root TP influences root length and indirectly affects other crop growth indicators such as shoot length, TK, TP, and DM, and root DM, TK, and TP. These crop growth indicators then affect potassium- and phosphorus-use efficiency, which further influences floodwater nutrient uptake. Therefore, flood depth creates a comprehensive loop impact on water quality, soil carbon sequestration and crop growth.

Various irrigation systems affect the non-point source nutrient losses, soil carbon sequestration, and productivity traits of rice crops. In addition to continuous flooding, numerous studies have highlighted water-saving techniques such as alternate wetting and drying irrigation, which conserve water, reduce greenhouse gas emissions, and enhance rice yield [34–36]. However, alternating wetting and drying also increases CO_2 emissions and can potentially adversely affect SOC [37–39]. The extreme weather will also amplify these detrimental effects in the agriculture [40]. Consequently, a climate-smart agriculture practice is needed to be resilient to climate change [41], and further research is warranted to assess the impacts of different irrigation methods on soil health, water quality, greenhouse gas emissions, and rice yield in the EAA.

5. Conclusions

Our two-year field study reveals how different flood depths can significantly impact water quality, outflow discharge, plant nutrient uptake, soil carbon dynamics, and yield. When averaged across years, flooded rice significantly reduced loadings of TSS, TN, TP, and TK by 40 %, 38 %, 36 %, and 32 %, respectively, compared with inflow water ($p < 0.001$). SOC increased annually at a rate of 3.85 %, 5.64 %, 6.86 %, and 6.86 %, in 5, 10, 15, and 20 cm flood-depth treatments, respectively; AOC decreased annually at rates of 11.75 %, 8.63 %, 20.07 %, and 8.48 % in 5, 10, 15, and 20 cm flood-depth treatments, respectively; and rice grain yield was 4488, 5103, 5450, and 5386 kg ha^{-1}, respectively. After a comparison of the non-point source losses, soil carbon sequestration, and crop yield, we recommend a flood depth of 15 cm within the EAA. We note, however, that such a depth might not be universally applicable, and that it may vary depending on the location and environmental conditions. Additionally, because we focus on continuous flooding throughout the growing season, greenhouse gas emissions should be considered by investigating the effects of alternating wetting and drying.

We report the effects of continuous flooding on non-point source nutrient losses, soil carbon sequestration, and crop growth by flood rice cultivation in the EAA. Recognizing and preserving these ecosystem services is important for sustainable agriculture, and for the overall well-being of natural and human systems in this region. Further research and policy initiatives could explore the benefits of flood rice cultivation within the context of broader environmental and societal goals.

Data availability statement

Data available on request from the authors.

CRediT authorship contribution statement

Yuchuan Fan: Writing – review & editing, Writing – original draft, Visualization, Methodology, Conceptualization. **Naba R. Amgain:** Writing – review & editing. **Abul Rabbany:** Writing – review & editing. **Noel Manirakiza:** Writing – review & editing. **Xue Bai:** Writing – review & editing. **Matthew VanWeelden:** Writing – review & editing. **Jehangir H. Bhadha:** Writing – review & editing, Supervision, Resources, Investigation, Funding acquisition, Conceptualization.

Declaration of competing interest

The authors declare that they have no known competing financial interests or personal relationships that could have appeared to influence the work reported in this paper.

Acknowledgments

This work was supported by the U.S. Environmental Protection Agency-Florida Department of Environmental Protection (319H), (Award No is AWD05732) and the Science and Technologies for Phosphorus Sustainability (STEPS) Center, a National Science Foundation Science and Technology Center (CBET-2019435), which is funding Dr. Jehangir H. Bhadha.

Appendix A. Supplementary data

Supplementary data to this article can be found online at https://doi.org/10.1016/j.csag.2024.100005.

References

[1] Y. Hu, et al., Bibliometric network analysis of crop yield gap research over the past three decades, Agriculture 13 (2023) 2105.
[2] J. Bhadha, et al., Evidence of soil health benefits of flooded rice compared to fallow practice, Sustain. Agric. Res. 7 (2018) 31–41.
[3] J.H. Bhadha, L. Trotta, M.T. VanWeelden, Trends in rice production and varieties in the Everglades agricultural area, Environ. Data Inf. Serv. 2016 (2016), 4-4.
[4] T. Ishida, et al., Effects of winter flooding on phosphorus dynamics in rice fields, Limnology 21 (2020) 403–413.
[5] M. Tootoonchi, et al., Reducing drainage water phosphorus concentration with rice cultivation under different water management regimes, Agric. Water Manag. 205 (2018) 30–37.
[6] J.H. Bhadha, A.L. Wright, G.H. Snyder, Everglades agricultural area soil subsidence and sustainability, Environ. Data Inf. Serv. (2020) 2020.

[7] J.H. Bhadha, T.A. Lang, S.H. Daroub, Influence of suspended particulates on phosphorus loading exported from farm drainage during a storm event in the Everglades Agricultural Area, J. Soils Sediments 17 (2017) 240–252.
[8] L.A. de Avila, et al., Rice water use efficiency and yield under continuous and intermittent irrigation, Agron. J. 107 (2015) 442–448.
[9] M. Chiba, et al., Improvement in rice grain quality by deep-flood irrigation and its underlying mechanisms, Jarq - Jpn. Agric. Res. Q. 51 (2017) 107–116.
[10] Y. Meng, S. Yu, Y. Yu, L. Jiang, Flooding depth and duration concomitantly influence the growth traits and yield of rice, Irrigat. Drain. (2021) 14.
[11] V. Anbumozhi, E. Yamaji, T. Tabuchi, Rice crop growth and yield as influenced by changes in ponding water depth, water regime and fertigation level, Agric. Water Manag. 37 (1998) 241–253.
[12] H.B. He, et al., The growth characteristics and yield potential of rice (Oryza sativa) under non-flooded irrigation in arid region, Ann. Appl. Biol. 168 (2016) 337–356.
[13] R. Ye, et al., Land-use effects on soil nutrient cycling and microbial community dynamics in the Everglades Agricultural Area, Florida, Commun. Soil Sci. Plant Anal. 40 (2009) 2725–2742.
[14] R.G. Allen, L.S. Pereira, D. Raes, M. Smith, FAO-crop Evapotranspiration-Guidelines for Computing Crop Water Requirements, FAO Irrigation and Drainage, 1998. Paper No.56Rome.
[15] FDEP, in: F.D.o.E. Protection (Ed.), Surface Water Quality Standards Classes, Uses, Critera, 2022.
[16] M.G. Uddin, S. Nash, A.I. Olbert, A review of water quality index models and their use for assessing surface water quality, Ecol. Indicat. 122 (2021) 107218.
[17] R. Schindelbeck, et al., Cornell University Comprehensive Assessment of Soil Health Laboratory Standard Operating Procedures, Cornell Univ., Ithaca, NY, 2016.
[18] E. Ben-Dor, A. Banin, Determination of organic matter content in arid-zone soils using a simple "loss-on-ignition" method, Commun. Soil Sci. Plant Anal. 20 (1989) 1675–1695.
[19] Y. Fan, et al., The global significance of abiotic factors affecting nitrate removal in woodchip bioreactors, Sci. Total Environ. (2022) 157739.
[20] Y. Fan, et al., Recycling silage leachate and biochar for improving nitrate removal by woodchip bioreactor, J. Environ. Manag. 345 (2023) 118735.
[21] N.R. Amgain, et al., From ground to grain: tracing phosphorus and potassium in flooded rice cultivar grown on histosols, Agriculture 12 (2022) 1250.
[22] M. Guardo, R.S. Tomasello, Hydrodynamic simulations of a constructed wetland in south Florida, JAWRA J. Am. Water Resour. Assoc. 31 (1995) 687–701.
[23] Y. Fan, et al., Characterizing the role of hydraulic retention time on nitrate removal indices in denitrifying bioreactors by nonlinear models, Environ. Technol. Innovat. 32 (2023) 103431.
[24] N.R. Amgain, Q. Zacharias, A. Rabbany, J.H. Bhadha, Effect of sulfur on rice water quality, nutrient uptake, and yields grown on shallow Histosols, J. Rice Res. Dev. 4 (2021) 324–330.
[25] Y. Fan, et al., Global significance of substrates for nitrate removal in denitrifying bioreactors revealed by meta-analysis, Engineering 21 (2023) 214–226.
[26] N.R. Amgain, et al., Developing soil health scoring indices based on a comprehensive database under different land management practices in Florida, Agrosystems, Geosci. Environ. 5 (2022) e20304.
[27] D. Qi, Q. Wu, J. Zhu, Nitrogen and phosphorus losses from paddy fields and the yield of rice with different water and nitrogen management practices, Sci. Rep. 10 (2020) 9734.
[28] J. Min, H. Zhang, W. Shi, Optimizing nitrogen input to reduce nitrate leaching loss in greenhouse vegetable production, Agric. Water Manag. 111 (2012) 53–59.
[29] X. Tan, et al., Effects of alternate wetting and drying irrigation on percolation and nitrogen leaching in paddy fields, Paddy Water Environ. 11 (2013) 381–395.
[30] A. Evald, et al., Soil attributes under different water management systems of rice paddies in the Amazonian savanna of Brazil, Rev. Caatinga 34 (2021) 640–649.
[31] J.-P. Métraux, H. Kende, The role of ethylene in the growth response of submerged deep water rice, Plant Physiol. 72 (1983) 441–446.
[32] A.L. Middelboe, S. Markager, Depth limits and minimum light requirements of freshwater macrophytes, Freshw. Biol. 37 (1997) 553–568.
[33] W. Dai, et al., Soil organic carbon dynamics shift by incorporating wheat straw in paddy soil in China, J. Environ. Qual. 52 (2023) 960–971.
[34] A. Pramono, et al., Alternate wetting and drying combined farmyard manure for reducing greenhouse gas while improving rice yield, IOP Conf. Ser. Earth Environ. Sci. 950 (2022) 012012.
[35] L.D. Phung, et al., Continuous sub-Irrigation with treated municipal wastewater for protein-rich rice production with reduced emissions of CH4 and N2O, Sci. Rep. 10 (2020) 5485.
[36] Y. Huang, et al., Leveraging the One Health Concept for Arsenic Sustainability, Eco-Environment & Health, 2024.
[37] J. Bhadha, et al., Capitalizing on carbon, Environ. Data Inf. Serv. (2023) 2023.
[38] J. Livsey, et al., Do alternative irrigation strategies for rice cultivation decrease water footprints at the cost of long-term soil health? Environ. Res. Lett. 14 (2019) 074011.
[39] J. Liu, et al., Nonmicrobial mechanisms dominate the release of CO2 and the decomposition of organic matter during the short-term redox process in paddy soil slurry, Eco-Environ. Health 2 (2023) 227–234.
[40] D. Xiao, D.L. Liu, X. Zhang, Y. Fan, Agricultural production in a warmer world: challenges and sustainable development strategies, Front. Earth Sci. 12 (2024) 1368149.
[41] Y. Lou, et al., Climate-smart Agriculture: Insights and Challenges, Elsevier, 2024 100003.